

Quantum error mitigation based on the Z-mixed-expression of the amplitude damping channel

Ting Li(李汀), Hangming Zhang(张航铭), Lingling Zheng(征玲玲), and Fei Li(李飞)
Citation: Chin. Phys. B, 2025, 34 (**12**): 124703. DOI: 10.1088/1674-1056/ae067c
http://cpb.iphy.ac.cn; http://iopscience.iop.org/cpb

What follows is a list of articles you may be interested in

Experimental study on characteristics of isopropanol ejection driven by electrohydrodynamics

Xi-Hao Zhang(张玺皓), Wen-Hua Wang (王文华), Cheng-Nan He(何承南), Yi-Chi Yao(姚奕弛), Bo-Yu Wang (王博宇), Xue-Hong Li(李学红), Zhi-Jian Wang(王智健), Chen Qiu(邱晨), Hai-Yi Sun(孙海轶), Yu-Xin Leng(冷雨欣), and Gang Xin(新刚)
Chin. Phys. B, 2025, 34 (**11**): 114701. DOI: 10.1088/1674-1056/addbcc

Evaporation of saline colloidal droplet and deposition pattern

Hong-Hui Sun(孙弘辉), Wei-Bin Li(李伟斌), Wen-Jie Ji(纪文杰), Guo-Liang Dai(戴国亮), Yong Huan(郇勇), Yu-Ren Wang(王育人), Ding Lan(蓝鼎)
Chin. Phys. B, 2020, 29 (**1**): 014701. DOI: 10.1088/1674-1056/ab5782

Capillary filling in closed-end nanotubes

Chen Zhao(赵晨), Jiajia Zhou(周嘉嘉), Masao Doi
Chin. Phys. B, 2018, 27 (**2**): 024701. DOI: 10.1088/1674-1056/27/2/024701

Instabilities of thermocapillary-buoyancy convection in open rectangular liquid layers

Huan Jiang(姜欢), Li Duan(段俐), Qi Kang(康琦)
Chin. Phys. B, 2017, 26 (**11**): 114703. DOI: 10.1088/1674-1056/26/11/114703

Critical condition for the transformation from Taylor cone to cone-jet

Wei Cheng (魏承), Gang Tie-Qiang (江铁强), Chen Li-Jie (陈立杰), Zhao Yang (赵阳)
Chin. Phys. B, 2014, 23 (**6**): 064702. DOI: 10.1088/1674-1056/23/6/064702

Quantum error mitigation based on the *Z*-mixed-expression of the amplitude damping channel

Ting Li(李汀)[1,†], Hangming Zhang(张航铭)[1,2], Lingling Zheng(征玲玲)[1], and Fei Li(李飞)[1]

[1] *School of Communications and Information Engineering, Nanjing University of Posts and Telecommunications, Nanjing* 210003, *China*
[2] *China Telecom Fujian Branch, Fuzhou* 350000, *China*

(Received 12 July 2025; revised manuscript received 14 September 2025; accepted manuscript online 15 September 2025)

In the field of quantum error mitigation, most current research separately addresses quantum gate noise mitigation and measurement noise mitigation. However, due to the typically high complexity of measurement noise mitigation methods, such as those based on estimating response matrices, the overall complexity of noise mitigation schemes increases when combining measurement noise mitigation with other quantum gate noise mitigation approaches. This paper proposes a low-complexity quantum error mitigation scheme that jointly mitigates quantum gate and measurement noise, specifically when measurement noise manifests as an amplitude damping channel. The proposed scheme requires estimating only three parameters to jointly mitigate both types of noise, whereas the zero-noise extrapolation method enhanced by response matrix estimation requires estimating at least six parameters under the same conditions.

Keywords: quantum error mitigation, measurement error mitigation, amplitude damping channel, low-complexity

PACS: 47.55.nb, 47.20.Ky, 47.11.Fg

DOI: 10.1088/1674-1056/ae067c **CSTR:** 32038.14.CPB.ae067c

1. Introduction

Quantum computing is advancing rapidly, with numerous noteworthy achievements to date. Nevertheless, we are still in the noisy intermediate-scale quantum (NISQ) era, where the number of qubits available in practical quantum devices remains limited.[1] Moreover, these quantum computers are susceptible to quantum noise during the execution of quantum tasks, leading to computational errors. To address this issue, many researchers have employed quantum error correction codes, which utilize ancillary qubits to correct errors in the output qubits.[2–6] While this approach significantly mitigates errors in quantum states, the overhead of quantum error correction scales polynomially with the number of output qubits, making it challenging to implement on current quantum computers with limited qubit counts.[6–8]

Consequently, the field of quantum error mitigation has emerged as a more practical alternative to quantum error correction.[7,8] Quantum error mitigation involves classical post-processing of the expectation values obtained from noisy quantum computers, aiming to bring these values closer to the ideal, noise-free expectations. Within a certain fault-tolerant threshold, current quantum computers can execute quantum circuits with nearly one hundred qubits and yield relatively reliable results through quantum error mitigation.

In the realm of quantum error mitigation, the terms "quantum error mitigation" and "quantum noise mitigation" are often used interchangeably. In practical quantum computing, there are two primary sources of noise: quantum gate noise, arising from the quantum gates in the circuit, and quantum measurement noise. Numerous solutions have been proposed by researchers to mitigate these noises. For quantum gate noise, techniques such as zero-noise extrapolation (ZNE), probabilistic error cancellation, and matrix product state methods have been developed.[9–13] For quantum measurement noise, approaches including bit-flip strategies, neural network-based methods, and modeling the measurement process as a Pauli channel followed by quantum–classical hybrid processing have been explored.[14–17] Among these methods, ZNE has become one of the most widely used gate error mitigation techniques. The main idea of ZNE is to artificially amplify the noise strength of a quantum circuit (e.g., through unitary folding), measure the noisy expectation values under different noise scaling factors λ, and then extrapolate to the zero-noise limit by fitting these results. Commonly used fitting functions include linear fitting, polynomial fitting, and exponential fitting. Depending on the choice of fitting function, the number of parameters to be estimated varies.

However, many existing noise mitigation schemes address either quantum gate noise or quantum measurement noise independently. For instance, the ZNE method specifically targets quantum gate noise by modeling it as a depolarizing channel. This technique involves measuring the expectation values $E(\lambda)$ of the original quantum circuit under different noise scaling factors λ through unitary folding, and

†Corresponding author. E-mail: lit@njupt.edu.cn

© 2025 Chinese Physical Society and IOP Publishing Ltd. All rights, including for text and data mining, AI training, and similar technologies, are reserved.

then extrapolating to the ideal noise-free expectation value $E(\lambda = 0)$ via function fitting. Nevertheless, this method does not account for quantum measurement noise. In practice, quantum measurement noise remains unchanged regardless of the number of unitary foldings, which can lead to suboptimal fitting results when quantum measurement noise is significant.

On the other hand, quantum measurement error mitigation methods, such as the bit-flip approach, represent the output probability distribution of a quantum computer as a vector $\boldsymbol{p}_{\text{obs}}$. By establishing a relationship between the observed and ideal probability distributions through a response matrix A, such that $\boldsymbol{p}_{\text{obs}} = A\boldsymbol{p}_{\text{ideal}}$, this method estimates the response matrix using known basis states and subsequently mitigates errors. While effective, the complexity of this approach grows exponentially with the number of qubits, making it impractical for large-scale implementations.

Moreover, in many quantum computing tasks, such as quantum machine learning, the focus is often on the expectation values of the outputs rather than the entire probability distribution. Although mitigating errors in the probability distribution can indirectly address expectation value errors, a more direct approach to mitigating expectation value errors could potentially reduce the complexity of the scheme.

Regarding quantum measurement noise, scholars have identified two primary sources: (i) decay of quantum states, such as transitions from the $|1\rangle$ state to the $|0\rangle$ state, and (ii) overlap of probability densities between quantum states, leading to measurement errors.[18] The second case has been addressed in the literature by modeling it as a Pauli channel.[19] However, the first case aligns more closely with the quantum amplitude damping channel, which is inherently unidirectional and irreversible, making it more complex to handle. This paper focuses on analyzing and addressing this specific scenario.

Based on the above discussion, this paper models the noise generated by quantum circuits as a depolarizing channel and the noise from quantum measurements as an amplitude damping channel.[20–22] We propose a quantum error mitigation scheme that jointly mitigates both quantum gate noise and quantum measurement noise. This scheme aims to ensure that the actual measured noisy expectation values of the quantum states output by the quantum circuit, after being subjected to these two types of noise, are as close as possible to the ideal noise-free expectation values. Additionally, since our scheme directly mitigates errors in the expectation values, its complexity is lower compared to the ZNE method enhanced by response matrix estimation, hereafter referred to as the response matrix-enhanced ZNE method. The so-called "response matrix-enhanced ZNE method" refers to a hybrid approach combining ZNE with measurement error mitigation based on response matrix estimation proposed by the authors in Ref. [12]. Specifically, our joint mitigation of quantum gate noise and quantum measurement noise requires only three parameters, whereas the enhanced ZNE method based on response matrix estimation requires at least six parameters.

We conducted comparative experiments with both the ZNE method and its enhanced version based on response matrix estimation. The results demonstrate that, in the presence of quantum measurement noise, the ZNE method performs poorly. While the enhanced ZNE method and our proposed scheme achieve similar error mitigation effects, our scheme exhibits lower complexity, highlighting its advantage.

2. The Z-mixed-stated expression of the amplitude damping channel

In this section, we analyze how the expectation values of quantum states change after passing through the depolarizing channel and the amplitude damping channel. Since a Pauli-X measurement can be implemented by applying a Hadamard gate before a Pauli-Z measurement at the end of a quantum circuit, and a Pauli-Y measurement can be realized by applying both a Hadamard gate and an $S^\dagger$ gate before a Pauli-Z measurement, all measurement operators can be decomposed into a combination of Pauli operators. Therefore, discussing the problem under Pauli-Z measurement is general and broadly applicable.

To avoid ambiguity, we first introduce several necessary conventions. In the following discussion, we consider the evolution of a single qubit, and in the output measurement stage, we always perform a Pauli-Z measurement on the quantum state.

First, the mathematical expression of the depolarizing channel is given by

$$\varepsilon_u(\rho) = p\rho + (1-p)\frac{I}{2}, \tag{1}$$

where ρ denotes the density matrix of the input quantum state, p is a parameter known as the depolarization rate, and I represents the identity operator.

The mathematical expression of the amplitude damping channel is given by

$$\varepsilon_m(\rho) = K_0\rho K_0^\dagger + K_1\rho K_1^\dagger, \tag{2}$$

where ρ is the density matrix of the input quantum state, $K_0 = \begin{pmatrix} 1 & 0 \\ 0 & \sqrt{1-\gamma} \end{pmatrix}$, $K_1 = \begin{pmatrix} 0 & \sqrt{\gamma} \\ 0 & 0 \end{pmatrix}$, and γ is a parameter characterizing the channel.

Inspired by Ref. [18] and for the convenience of subsequent analysis, we reformulate the original expression of the amplitude damping channel, namely Eq. (2), into its Z-mixed-state expression

$$\varepsilon_m(\rho) = \frac{\mathrm{tr}(Z\rho) + 2\mathrm{tr}(\kappa\rho)}{\mathrm{tr}(Z\rho) + \mathrm{tr}(\kappa\rho)} K_0\rho K_0^\dagger + z_0, \tag{3}$$

where $z_0 = K_1\rho K_1^\dagger - \frac{\mathrm{tr}(\kappa\rho)}{\mathrm{tr}(Z\rho)+\mathrm{tr}(\kappa\rho)} K_0\rho K_0^\dagger$ and $\kappa = \begin{pmatrix} 0 & 0 \\ 0 & \gamma \end{pmatrix}$. After reformulating the original expression of the quantum amplitude damping channel into its Z-mixed-state expression, the advantage lies in the fact that $\mathrm{tr}(Zz_0) = 0$. This property allows us to easily derive the relationship between its expectation value and the ideal value under Pauli-Z measurement.

The proof of $\mathrm{tr}(Zz_0) = 0$ is given as follows:

$$\begin{aligned} \mathrm{tr}(Zz_0) &= \mathrm{tr}\left[Z\left(K_1\rho K_1^\dagger - \frac{\mathrm{tr}(\kappa\rho)}{\mathrm{tr}(Z\rho)+\mathrm{tr}(\kappa\rho)} K_0\rho K_0^\dagger\right)\right] \\ &= \mathrm{tr}\left(K_1^\dagger Z K_1\rho - \frac{\mathrm{tr}(\kappa\rho)}{\mathrm{tr}(Z\rho)+\mathrm{tr}(\kappa\rho)} K_0^\dagger Z K_0\rho\right). \quad (4) \end{aligned}$$

Through calculation, we find that $K_0^\dagger Z K_0 = Z + \kappa$ and $K_1^\dagger Z K_1 = \kappa$. Therefore,

$$\begin{aligned} \mathrm{tr}(Zz_0) &= \mathrm{tr}\left[\kappa\rho - \frac{\mathrm{tr}(\kappa\rho)}{\mathrm{tr}(Z\rho)+\mathrm{tr}(\kappa\rho)}(Z+\kappa)\rho\right] \\ &= \mathrm{tr}(\kappa\rho) - \frac{\mathrm{tr}(\kappa\rho)}{\mathrm{tr}(Z\rho)+\mathrm{tr}(\kappa\rho)}\mathrm{tr}(Z\rho+\kappa\rho) \\ &= \mathrm{tr}(\kappa\rho) - \mathrm{tr}(\kappa\rho) = 0. \quad (5) \end{aligned}$$

Therefore, in the Z-mixed-state expression of the amplitude damping channel, the expectation value of the z_0 term under the Pauli-Z measurement is zero. Utilizing this property, we can easily determine how the expectation value of a quantum state changes after passing through the quantum amplitude damping channel

$$\mathrm{tr}(Z\varepsilon_m(\rho)) = \mathrm{tr}\left(Z\left(\frac{\mathrm{tr}(Z\rho)+2\mathrm{tr}(\kappa\rho)}{\mathrm{tr}(Z\rho)+\mathrm{tr}(\kappa\rho)} K_0\rho K_0^\dagger + z_0\right)\right). \quad (6)$$

Using the previously obtained results $K_0^\dagger Z K_0 = Z + \kappa$ and $\mathrm{tr}(Zz_0) = 0$, we obtain

$$\mathrm{tr}(Z\varepsilon_m(\rho)) = \mathrm{tr}(Z\rho) + 2\mathrm{tr}(\kappa\rho). \quad (7)$$

It can be observed that the relationship between the expectation value of a quantum state after passing through the quantum amplitude damping channel and its ideal expectation value depends on the quantum state itself, as reflected in the $\mathrm{tr}(\kappa\rho)$ term. This also suggests that quantum noise mitigation under the quantum amplitude damping channel may require estimating certain information about the quantum state itself.

Next, we use the Z-mixed-state expression of the amplitude damping channel to analyze the relationship between the measured expectation value and the ideal expectation value when a quantum state first passes through the depolarizing channel and then through the quantum amplitude damping channel

$$\begin{aligned} \mathrm{tr}(Z\varepsilon_m(\varepsilon_u(\rho))) &= \mathrm{tr}\left[Z\varepsilon_m\left(p\rho + (1-p)\frac{I}{2}\right)\right] \\ &= \mathrm{tr}\left[Z\varepsilon_m(p\rho) + Z\varepsilon_m\left((1-p)\frac{I}{2}\right)\right]. \quad (8) \end{aligned}$$

In Eq. (8), the first term on the right-hand side of the second equality may be substituted with Eq. (7), yielding $p[\mathrm{tr}(Z\rho) + 2\mathrm{tr}(\kappa\rho)]$. For the second term, the presence of the identity operator allows straightforward computation. Finally, we obtain

$$\mathrm{tr}(Z\varepsilon_m(\varepsilon_u(\rho))) = p\,\mathrm{tr}(Z\rho) + 2p\,\mathrm{tr}(\kappa\rho) + (1-p)\gamma. \quad (9)$$

If we assume $\rho = \begin{pmatrix} \rho_{11} & \rho_{12} \\ \rho_{21} & \rho_{22} \end{pmatrix}$ and substitute it into the equation, we obtain

$$\mathrm{tr}(Z\varepsilon_m(\varepsilon_u(\rho))) = p\,\mathrm{tr}(Z\rho) + 2p\rho_{22}\gamma + (1-p)\gamma. \quad (10)$$

The above equation describes the relationship between the actual measured expectation value and the ideal expectation value after a quantum state passes through the depolarizing channel followed by the quantum amplitude damping channel. This relationship will guide the design of our subsequent quantum noise mitigation scheme. It can be observed that the relationship between the measured expectation value and the ideal expectation value is a function of three parameters: p, ρ_{22}, and γ.

In addition, one may wonder whether the presence of a dephasing channel affects the results. For a dephasing channel, the process can be expressed as

$$\varepsilon(\rho) = q\rho + (1-q)Z\rho Z, \quad (11)$$

where ρ is the density matrix of the input quantum state, q denotes the dephasing probability, and Z is the Pauli-Z operator. When measuring under the Pauli-Z basis, we obtain

$$\mathrm{tr}(Z\varepsilon(\rho)) = \mathrm{tr}\{Z[q\rho + (1-q)Z\rho Z]\} = \mathrm{tr}(Z\rho). \quad (12)$$

Since a dephasing channel leaves the expectation values under Pauli-Z measurement unchanged, the measured expectation value remains identical to the ideal one. Therefore, dephasing noise does not influence the analysis, and the proposed mitigation scheme remains valid in the presence of dephasing channels.

3. Quantum error mitigation based on the Z-mixed-state expression of the amplitude damping channel

As shown in the previous section, there are three parameters p, ρ_{22}, and γ that need to be estimated. Our subsequent scheme focuses on estimating these three parameters and is referred to as the QEM-ZMSEAD scheme.

Before introducing the scheme in detail, we first clarify the noise modeling adopted in this approach. We begin by defining the notations to be used.

Assume that the quantum circuit implemented on a real quantum device is denoted by U, and the initial quantum state

of a specific circuit is $|0\rangle$, denoted by ρ_0. After evolving through the quantum circuit U, the quantum state becomes ρ. The circuit U consists of a sequence of quantum gates, and we assume that the noise introduced by these gates can be modeled as a depolarizing channel, denoted by ε_u. After passing through the depolarizing channel, the state ρ is transformed into $\varepsilon_u(\rho)$.

It should be emphasized that in our noise modeling, the noise from all quantum gates in the circuit — both single-qubit and multi-qubit gates — is treated as an effective overall depolarizing channel. In this sense, the depolarizing parameter p captures the collective effect of the entire quantum circuit rather than individual gates. This treatment allows us to derive and analyze the ZMSEAD-based mitigation scheme in a unified manner while keeping the parameter estimation procedure simple and low in complexity.

In the quantum measurement stage, measurement noise may occur, leading to state relaxation, i.e., the quantum state may collapse from $|1\rangle$ to $|0\rangle$. This behavior is physically analogous to that of the amplitude damping channel, and we thus model it using a quantum amplitude damping channel, denoted by ε_m. The final measured quantum state is denoted by $\varepsilon_m(\varepsilon_u(\rho))$, and the actual measured expectation value is denoted by $\mathrm{tr}(Z\varepsilon_m(\varepsilon_u(\rho)))$.

Figure 1 illustrates the overall noise modeling. Next, we introduce the detailed procedure of the proposed scheme, as illustrated in steps 1 to 3 of Fig. 1.

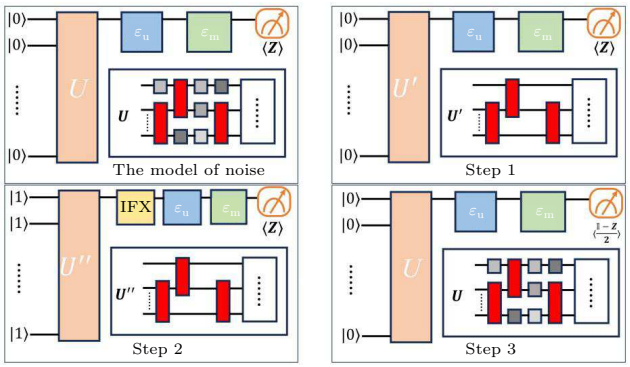


Fig. 1. Quantum noise model assumptions and the steps of QEM-ZMSEAD method.

Step 1 involves constructing a modified quantum circuit for estimating the gate noise parameter p in the original circuit U, as well as the measurement noise parameter γ. This reconstructed circuit, denoted as U^*, retains all the two-qubit gates from the original circuit U while discarding all single-qubit gates.

In real quantum hardware, the noise introduced by single-qubit gates is typically negligible compared to that from two-qubit gates, particularly CNOT gates. Therefore, we assume that the noise level in the reconstructed circuit U^* closely approximates that of the original circuit U.[12] This observation was also noted by the authors in Ref. [12], where it was stated that

$$\varepsilon_u(\rho) = p\rho + (1-p)\frac{I}{2}, \tag{13}$$

$$\varepsilon_{u^*}(\rho) = p^*\rho + (1-p^*)\frac{I}{2}, \tag{14}$$

$$p^* \approx p. \tag{15}$$

In other words, the depolarizing noise parameters induced by gate operations in both circuits are nearly identical, and we can approximately treat them as equal.

We then prepare the quantum state ρ_0 as the input state and evolve it through the reconstructed circuit U^*, followed by measurement. Since the initial state is $|0\rangle$, and U^* consists solely of CNOT gates — which only flip the target qubit when the control qubit is in the $|1\rangle$ state — the initial state $|0\rangle$ should remain unchanged after passing through the circuit U^*. Therefore, the quantum state after evolution is still ρ_0.

The resulting measured expectation value is denoted as

$$\langle z\rangle_0 = \mathrm{tr}(Z\varepsilon_m(\varepsilon_{u^*}(\rho_0))). \tag{16}$$

Since $\rho_0 = \begin{pmatrix} 1 & 0 \\ 0 & 0 \end{pmatrix}$, and the element at the ρ_{22} position is 0, substituting into Eq. (10) yields

$$\langle z\rangle_0 = \mathrm{tr}(Z\varepsilon_m(\varepsilon_{u^*}(\rho_0))) = p^*\mathrm{tr}(Z\rho_0) + (1-p^*)\gamma. \tag{17}$$

Given that we deliberately use ρ_0 as the input state, its ideal measurement expectation value is 1. Substituting this into Eq. (17) leads to

$$\langle z\rangle_0 = p + (1-p)\gamma. \tag{18}$$

This equation contains two unknown variables, which cannot be solved directly. In the next step, we construct another equation to resolve these variables.

Step 2 involves constructing a second modified quantum circuit, denoted as U^{**}, for estimating the same gate noise parameter p and measurement noise parameter γ. The structure of U^{**} is similar to that of U^*; it also preserves all the CNOT gates from the original circuit U but differs in that the input quantum state is changed from $|0\rangle$ to $|1\rangle$. Moreover, an IFX gate (a conditional Pauli-X gate ensuring the $|1\rangle$ output) is appended at the end of the circuit.

We now elaborate on the rationale behind this design. In step 1, because the circuit was composed entirely of CNOT gates and the input state consisted entirely of $|0\rangle$, the output state theoretically remains unchanged after passing through the circuit U^*, i.e., it remains $|0\rangle$, and no additional operations are required. This is due to the fact that a CNOT gate only flips the target qubit when the control qubit is in the $|1\rangle$ state.

However, in the current case, where the input state is $|1\rangle$, the output state after passing through an all-CNOT circuit could potentially change, it may become either $|0\rangle$ or $|1\rangle$, depending on the number and arrangement of the CNOT gates.

Hence, we introduce the IFX gate to ensure that the output state remains $|1\rangle$.

Implementing the IFX gate in practice is straightforward. It involves preparing a small number of quantum states and performing repeated measurements. If the measured expectation value is greater than zero, it indicates that the input state $|1\rangle$ has likely been flipped to $|0\rangle$ due to the action of multiple CNOT gates, because the ideal measurement expectation of $|0\rangle$ is 1. In this case, we append a Pauli-X gate to flip the state from $|0\rangle$ back to $|1\rangle$.

This process assumes that the magnitude of measurement noise is not excessively large, that is, not strong enough to degrade most of the $|1\rangle$ states in the circuit into $|0\rangle$.

Conversely, if the expectation value is less than zero, we do not apply any further operations, since the output state is likely already $|1\rangle$, whose ideal measurement expectation value is -1.

After ensuring that the output remains $|1\rangle$, we proceed with the measurement, and the obtained expectation value is

$$\langle z\rangle_1 = \mathrm{tr}\left(Z\varepsilon_m\left(\varepsilon_{u^{**}}\left(\rho_1\right)\right)\right). \tag{19}$$

Substituting into Eq. (14), we obtain

$$\langle z\rangle_1 = p\,\mathrm{tr}\left(Z\rho_1\right) + 2p\,\mathrm{tr}\left(\kappa\rho_1\right) + (1-p)\,\gamma. \tag{20}$$

Since the ideal measurement expectation value of $|1\rangle$ is -1, substituting this into the equation above yields

$$\langle z\rangle_1 = -p + (1+p)\,\gamma. \tag{21}$$

By solving Eqs. (18) and (21) simultaneously, we obtain

$$\gamma = \frac{\langle z\rangle_0 + \langle z\rangle_1}{2}, \tag{22}$$

$$p = \frac{\langle z\rangle_0 - \langle z\rangle_1}{2\left(1-\gamma\right)}. \tag{23}$$

In this way, we complete the estimation of the parameters p and γ. In the next step, we design a procedure to estimate the parameter ρ_{22}.

Step 3 involves constructing a reconstruction quantum circuit to estimate partial parameters of the output quantum state ρ. This circuit is identical to U itself, and the output expectation value is measured based on a linear combination of the identity operator and the Pauli-Z operator. Specifically, we employ the observable $\frac{I-Z}{2}$, where Z is the Pauli-Z operator and I denotes the identity operator. In practice, the implementation of this operator is straightforward. When performing measurements with respect to I, its outcome is always 1, as

$$\mathrm{tr}\left(I\rho\right) = \mathrm{tr}\left(\rho\right) = 1. \tag{24}$$

Therefore, the measurement with respect to $\frac{I-Z}{2}$ can be easily realized via a standard Pauli-Z measurement followed by simple arithmetic.

Suppose the quantum circuit outputs a quantum state $\rho = \begin{pmatrix}\rho_{11} & \rho_{12}\\ \rho_{21} & \rho_{22}\end{pmatrix}$. After undergoing both the depolarizing channel and the amplitude damping channel, the resulting density matrix becomes

$$\rho^* = \varepsilon_m\left(\varepsilon_u\left(\rho\right)\right) = \begin{pmatrix} *_1 & *_2 \\ *_3 & \frac{(1-\gamma)(1-p)}{2} + p\left(1-\gamma\right)\rho_{22}\end{pmatrix}, \tag{25}$$

where the asterisks $*$ denote elements that are irrelevant to the current analysis, as will be clarified shortly.

Now, we apply the operator $\frac{I-Z}{2}$ for measurement. The outcome of this measurement is given by

$$\left\langle \frac{I-Z}{2}\right\rangle = \mathrm{tr}\left(\frac{I-Z}{2}\rho^*\right). \tag{26}$$

Since $\frac{I-Z}{2} = \begin{pmatrix}0 & 0\\ 0 & 1\end{pmatrix}$, it effectively extracts the bottom-right element of ρ^*. This explains why we denoted the other elements with $*$: they do not contribute to the measurement result. Thus, we have

$$\left\langle \frac{I-Z}{2}\right\rangle = \frac{(1-\gamma)(1-p)}{2} + p\left(1-\gamma\right)\rho_{22}. \tag{27}$$

Here, the left-hand side corresponds to the experimentally obtained value, while the parameters p and γ on the right-hand side have already been estimated. Therefore, the only unknown in this equation is ρ_{22}, which can now be solved.

Once the parameters p, γ, and ρ_{22} have all been estimated, noise mitigation can be performed according to Eq. (14). The final noise mitigation expression is given by

$$\langle z\rangle_{\mathrm{mitigated}} = \frac{\langle z\rangle_{\mathrm{unmitigated}} - 2p\gamma\rho_{22} - (1-p)\,\gamma}{p}, \tag{28}$$

where $\langle z\rangle_{\mathrm{unmitigated}}$ denotes the raw expectation value obtained from measuring the noisy quantum circuit U, and p, γ, and ρ_{22} are the previously estimated noise parameters.

4. Numerical experiments

In this section, we present numerical experiments to verify the effectiveness of the proposed QEM-ZMSEAD method. All simulations are carried out using the Pennylane quantum computing platform. To evaluate the performance of the method, we employ a Trotter-step quantum circuit as the test circuit, as illustrated in Fig. 2.[23,24]

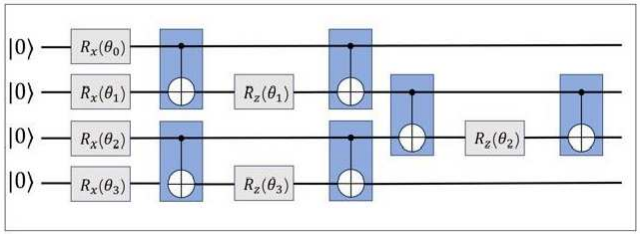


Fig. 2. A Trotter step quantum circuit.

For baseline comparisons, we consider two widely adopted approaches: the ZNE method and the response matrix-enhanced ZNE method. To facilitate more intuitive visualization, the expectation value is directly used as the evaluation metric in this section.

We simulate the Trotter-step quantum circuit in Pennylane and incorporate quantum noise as defined in Eqs. (1) and (2).

First, we fix the depolarizing channel parameter at $p = 0.9$ and the amplitude damping channel parameter at $\gamma = 0.2$. Under these noise settings, we compare the performance of our proposed method with that of the ZNE method. For the ZNE baseline, we adopt an exponential fitting variant, using the noise scaling factors $\lambda = \{1, 3\}$.

In the Trotter-step quantum circuit, the rotation angle of the R_z gates is fixed at -0.2, while the rotation angle of the R_x gates varies from 0 to 3 in increments of 0.2. All rotation parameters are expressed in radians. For example, a value such as 0.4 denotes 0.4 radians rather than 0.4π. Throughout all experiments in this work, the rotation gate angles are consistently specified in radians. This configuration results in 16 distinct Trotter-step circuits, each producing a unique ideal expectation value. The number of measurement shots is set to 1000, and a Pauli-Z measurement is applied to the final qubit.

For each configuration, 30 independent experimental runs are conducted, yielding a total of 1440 data points. In all figures presented in this section, the vertical axis labeled "Value" represents the measured expectation value of the quantum state, which is computed as

$$\frac{N_0 \times 1 + N_1 \times (-1)}{N_{\text{shots}}}, \tag{29}$$

where N_0 and N_1 denote the numbers of measurement outcomes in the $|0\rangle$ and $|1\rangle$ states, respectively, and N_{shots} is the total number of measurement shots. The experimental results are illustrated in Fig. 3.

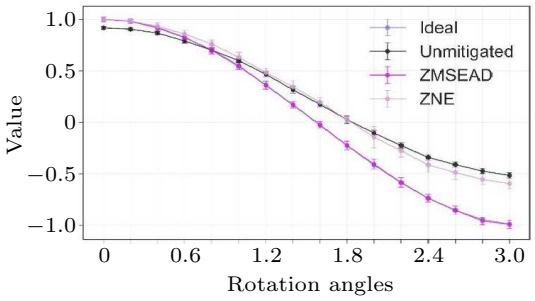


Fig. 3. Experimental results of Trotter step quantum circuits with different rotation angles.

From Fig. 3, it can be observed that the expectation values mitigated using the QEM-ZMSEAD method closely align with the ideal values, with deviations attributable primarily to experimental precision. When the quantum measurement noise is modeled as a quantum amplitude damping channel and the rotation angle of the R_x gate is near zero, the ideal quantum state contains a large $|0\rangle$ component. Since $|0\rangle$ is unaffected by amplitude damping, the quantum state is effectively influenced only by the depolarizing gate noise. Therefore, under such conditions, the ZNE method remains effective for noise mitigation, as shown in the cases with rotation angles of 0, 0.2, and 0.4 in Fig. 3.

However, as the R_x gate angle increases, the ideal quantum state evolves and gradually contains more $|1\rangle$ components, which are affected by the amplitude damping channel. In such cases, the $|1\rangle$ state may decay to $|0\rangle$, potentially resulting in measured expectation values exceeding the ideal values. Consequently, the unmitigated results may lie above the ideal expectation curve. Since the ZNE method does not account for quantum measurement noise, its mitigation performance deteriorates under these circumstances.

Next, we fix the rotation angle of the R_x gate to π, so that the ideal expectation value of the Trotter step circuit becomes -1, which facilitates subsequent analysis. We vary the quantum measurement noise parameter γ in the amplitude damping channel to values of 0, 0.1, 0.3, and 0.5. For each case, we apply both the QEM-ZMSEAD and ZNE methods for noise mitigation. Each scenario is repeated 30 times, resulting in 360 data points in total. The results are shown in Fig. 4.

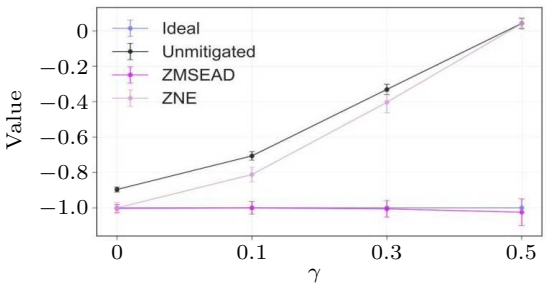


Fig. 4. Experimental results under different noise parameters.

From Fig. 4, it is evident that the QEM-ZMSEAD method effectively mitigates both gate and measurement noise. In contrast, the ZNE method loses stability and becomes ineffective as the measurement noise increases. When $\gamma = 0.5$, and the ideal expectation value is -1, the extrapolated result from ZNE approaches 0, exhibiting a significant deviation and becoming nearly indistinguishable from the unmitigated outcome. This indicates the failure of the ZNE method in such a complex noise environment.

The previous experiments have focused on comparisons with the standard ZNE method. We now compare the QEM-ZMSEAD method with the response matrix-enhanced zero-noise extrapolation method. The experimental circuit remains a 4-qubit Trotter step circuit with the R_x gate angle again set to π, implying an ideal expectation value of -1 for the circuit, which aids in performance comparison.

We introduce amplitude damping noise in the measurement process with $\gamma = 0.2$, and depolarizing gate noise with $p = 0.9$ remains unchanged. Each method is evaluated over 30 trials, and the experimental results are presented in Fig. 5.

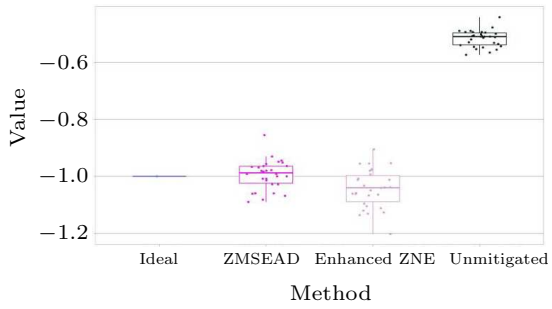


Fig. 5. Experimental results for comparing with enhanced ZNE.

The results show that the QEM-ZMSEAD method achieves noise mitigation performance comparable to that of the response matrix-enhanced ZNE method. By increasing the number of fitting points in ZNE, the two methods can achieve near-identical performance within the margin of error. However, it is noteworthy that the expectation value obtained from the enhanced ZNE method falls below -1, which is theoretically infeasible. In practice, the prediction range can always be constrained, but in this study, we do not apply such constraints to better evaluate the raw mitigation capabilities of each method in terms of the deviation from the ideal value.

Similarly, while QEM-ZMSEAD could also include output range constraints in practical applications, this paper focuses on assessing its original experimental performance without additional restrictions.

Finally, we apply the QEM-ZMSEAD method to a quantum machine learning task under noisy conditions to evaluate its performance enhancement. The chosen task involves optimizing the expectation value of a quantum circuit's output to converge to -1 through parameter updates, a common objective in classification tasks. Here, the loss function is defined as

$$L(\theta) = \left[\langle 0|U(\theta)^{\dagger} Z_1 U(\theta)|0\rangle - (-1)\right]^2, \tag{30}$$

where Z_1 denotes the Pauli-Z measurement on the first qubit, $|0\rangle$ represents the initial ground state, and $U(\theta)$ is the parameterized quantum circuit with θ being the rotation gate parameters.

In the noise simulation, we introduce a quantum amplitude damping channel with parameter $\gamma = 0.2$ to model measurement noise and a depolarizing channel with parameter $p = 0.9$ to account for gate noise, while keeping all other conditions unchanged.

The experiment was repeated five times, and the corresponding loss curves are shown in Fig. 6.

In the figure, the shaded region represents the range of all possible outcomes, while the solid curve indicates the average result. Without any error mitigation, the loss curve exhibits unstable fluctuations and fails to converge. In contrast, after applying QEM-ZMSEAD, the loss curve demonstrates significantly improved convergence, highlighting the practical utility of our method in realistic noisy quantum computations.

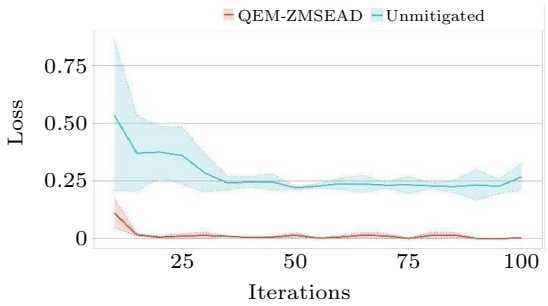


Fig. 6. Curves of the loss function with and without error mitigation.

5. Complexity analysis

This subsection primarily discusses and compares the complexity of the QEM-ZMSEAD scheme and the complexity of the ZNE method enhanced by the estimated response matrix approach. To facilitate a comparison under consistent conditions, the analysis is conducted based on a single-qubit scenario. In the case of one qubit, the complexity of the ZNE method enhanced by the estimated response matrix approach consists of two components: the number of computational parameters required for the estimated response matrix method and the number of parameters to be estimated for the ZNE method itself. Regarding the computational parameter count of the estimated response matrix method, the number of response matrix parameters amounts to $2 \times 2 = 4$ parameters. For gate noise mitigation, the ZNE method requires at least two parameters for linear fitting, and more typically three or more when fitting with exponential or polynomial functions for better mitigation performance. Specifically, in the case of a single qubit, the response matrix method has a dimension of 2×2 requiring the estimation of $2 \times 2 = 4$ parameters. For ZNE, even the simplest linear fitting function $f(\lambda) = a\lambda + b$ requires estimating two additional parameters a and b. Therefore, the response matrix-enhanced ZNE method requires at least $4 + 2 = 6$ parameters. If higher-order polynomial fitting functions are used in ZNE, the number of parameters to be estimated can increase further.

In summary, the enhanced ZNE method requires at least six parameters, and more than eight are often needed for effective noise suppression. In contrast, the QEM-ZMSEAD method can jointly mitigate both gate and measurement noise by estimating only three parameters, demonstrating its lower complexity.

The reason QEM-ZMSEAD can achieve effective noise mitigation with such low complexity is that it is based on the

ZMSEAD expression, which extracts key noise characteristics through careful analysis of the quantum noise model. This insight enables the design of an efficient mitigation strategy that significantly reduces overall complexity.

Data availability statement

The data that support the findings of this study are openly available in Science Data Bank at the following link https://doi.org/10.57760/sciencedb.j00113.00252.

Acknowledgment

Project supported by the National Natural Science Foundation of China (Grant No. 62271265).

References

[1] Preskill J 2018 *Quantum* **2** 79
[2] Fowler A G, Mariantoni M, Martinis J M and Cleland A N 2012 *Phys. Rev. A* **86** 032324
[3] Horsman D, Fowler A G, Devitt S and Munro W J 2012 *New J. Phys.* **14** 123011
[4] Bacon D 2006 *Phys. Rev. A* **73** 012340
[5] Knill E, Laflamme R and Viola L 2000 *Phys. Rev. Lett.* **84** 2525
[6] Gottesman D 2002 *Proc. Symp. Appl. Math.* **58** 221
[7] Suzuki Y, Endo S, Fujii K, Mitarai K and Nakajima T 2022 *PRX Quantum* **3** 010345
[8] Endo S, Benjamin S C and Li Y 2018 *Phys. Rev. X* **8** 031027
[9] Giurgica-Tiron T, Hindy Y, LaRose R, Mari A and Zeng W J 2020 *IEEE International Conference on Quantum Computing and Engineering*, October 12-16, 2020, Denver, USA, pp. 306
[10] Li Y and Benjamin S C 2017 *Phys. Rev. X* **7** 021050
[11] Temme K, Bravyi S and Gambetta J M 2017 *Phys. Rev. Lett.* **119** 180509
[12] Urbanek M, Nachman B, Pascuzzi V R, He A, Bauer C W and de Jong W A 2021 *Phys. Rev. Lett.* **127** 270502
[13] Guo Y and Yang S 2022 *PRX Quantum* **3** 040313
[14] Smith A W R, Khosla K E, Self C N and Kim M S 2021 *Sci. Adv.* **7** eabi8009
[15] Hicks R, Kobrin B, Bauer C W and Kaplan T 2022 *Phys. Rev. A* **105** 012419
[16] Kwon H and Bae J 2020 *IEEE Trans. Comput.* **70** 1401
[17] Zhao R S, Ma H Y, Cheng T, Wang S and Fan X K 2024 *Chin. Phys. B* **33** 040304
[18] Nachman B, Urbanek M, de Jong W A and Bauer C W 2020 *Quantum Inf.* **6** 84
[19] Zhang H, Li T and Li F 2024 *Quantum Inf. Process.* **23** 213
[20] Yeo Y and Skeen A 2003 *Phys. Rev. A* **67** 064301
[21] Fletcher A S, Shor P W and Win M Z 2008 *IEEE Trans. Inf. Theory* **54** 5705
[22] Chessa S and Giovannetti V 2021 *Commun. Phys.* **4** 22
[23] Smith A, Kim M S, Pollmann F and Knolle J 2019 *Quantum Inf.* **5** 106
[24] Suzuki M 1976 *Commun. Math. Phys.* **51** 183